

## IDETC2025-XXXX

### TEXTURE DESIGN FOR DIVERSE VIRTUAL TOUCH SENSATIONS: PERCEPTUAL BREADTH OF PARAMETER-DRIVEN TURING PATTERNS

MacKenzie Harnett<sup>1,†</sup>, Pijuan Yu<sup>1,†</sup>, Rebecca Friesen<sup>3,\*</sup>,

<sup>1</sup>Texas A&M University, College Station, TX

#### **ABSTRACT**

*Surface haptic technology reintegrates the sense of touch into virtual interactions on touchscreen devices, enhancing social interactions, educational tools, and daily screen tasks. Despite its clear benefits, this technology remains niche and guidelines for designing diverse and compelling touch sensations are lacking. The ability to easily generate content for and the existence of an established library of unique sensations and interactions may make the adoption of this technology more appealing to the average touchscreen user and for a broader range of mainstream applications. This study looks at the potential for parameter-driven reaction-diffusion algorithms to generate distinct, user-adjustable, and responsive texture stimuli.*

*Our user study investigating the perceived dissimilarity of a representative set of reaction-diffusion textures found that there is limited potential for reaction-diffusion textures in virtual texture spaces when using a friction-modulating display as the delivery platform, as perceived dissimilarity has a weak association with both control parameters. Control parameters had a stronger association with similarity ratings for real 3D printed textures, suggesting that Turing patterns are more suitable to diverse and intentional texture generation for alternative haptic surface displays (e.g. shape displays).*

*These results can inform how reaction-diffusion algorithms can be best leveraged to contribute to visual or tactile texture generation pipelines and spaces.*

**Keywords:** Texture perception, Reaction-diffusion, Multi-dimensional scaling analysis

#### **1. INTRODUCTION**

One of the most common experiences involving tactile feedback when evaluating an object or environment is through the interpretation of textures. Due to increasing dependencies on

touchscreen technologies and digital platforms as a primary mode of social communication, this way of interacting with spaces has been neglected. When considering practical applications, the lack of high-resolution tactile feedback means that a promising method of encoding information on digital platforms is unrealized.

There are a few methods for conveying virtual haptic texture information, including friction modulation or vibrotactile feedback. While these technologies show promise in reintroducing highly realistic textures onto digital platforms, they, and the methods used to generate these textures, lack mainstream implementations and are generally inaccessible to average touchscreen users. This may create a sort of issue where the technology is difficult to adopt because content-creation using the technology is so inaccessible, limiting its usefulness to haptic experts with access to the equipment, expertise, and resources necessary to make tactile graphics.

This paper presents a pipeline by which users can create parameter-driven tactile textures using a reaction-diffusion algorithm, which is the mechanism by which Turing patterns emerge. As a basis for how cellular organisms and natural patterns organize themselves, we hypothesized that reaction-diffusion might be an accessible method by which a breadth of highly distinct textures could be generated. However, we first needed to verify the physical and virtual design spaces in which reaction-diffusion textures span to assess whether it was practical or possible to map the controllable parameters to intuitive tactile analogs (e.g., smoothness-roughness).

We conducted a human-subject study in which participants rated the dissimilarity of a series of textures that spanned a representative range of possible reaction-diffusion outputs. Our study examines three possible implementations of these reaction-diffusion textures to determine the breadth of the resultant design spaces and the efficacy of using the algorithm for texture content generation. These three implementations include:

- Perception of a texture when using visual feedback.

<sup>†</sup>Joint first authors

\*Corresponding author: rfriesen@tamu.edu

Documentation for asmeconf.cls: Version 1.40, July 20, 2025.

- Perception of a physical texture when using tactile feedback.
- Perception of a virtual texture when using tactile feedback.

These implementations isolate individual senses to assess the potential of reaction-diffusion textures to convey information using *only* visual or *only* tactile feedback and the space and dimensions they span using those different feedback modes.

We believe that parameter-driven textures have the potential to make content generation easier for the end user, respond to user behaviors, and expand the library of available textures in the virtual texture design space. Ultimately, we want to establish the appropriateness of reaction-diffusion textures for this application and recommend how they can be used in this space.

## 2. BACKGROUND

Our work is informed by broader research into methods for generating unique, engaging, and responsive haptic sensations on surface haptic displays. This work is primarily inspired by existing research in different virtual texture generation methods and the perceptual spaces in which these textures span.

### 2.1. Texture Generation Methods

Virtual textures can be prepared by mechanical measurements of texture topology information when traced by an intermediary tool [1–4] or the fingertip [5, 6] using force, acceleration data, or displacement measurements of the tool along the surface. Highly realistic texture data often require mechanical measurement equipment that would be prohibitively expensive and/or require expert assistance. To avoid this, it is possible to generate novel textures by interpolating or modifying existing texture data [1, 3]; but these methods of generating textures require those initial measurements and do not necessarily adapt to user behavior; that is, these textures cannot adapt to variable swipe speed, force, or direction—behaviors that can significantly vary the impression of a texture during tactile exploration [7]. In contrast to textures generated using mechanical measurements, some procedurally generated textures can be created at runtime and thus can change in response to user behavior. These types of texture graphics have previously been generated using noise [8] or stochastic models [9, 10]. An opportunity to contribute to this growing library of parameter-driven textures is using parameter-driven “reaction-diffusion” textures, which may represent an accessible texture generation pipeline capable of creating distinct textures in mono-visual and -tactile contexts.

### 2.2. Reaction Diffusion Textures

Reaction-diffusion patterns were first described in Alan Turing’s seminal article describing the mechanisms by which biological patterns emerge [11]. These “Turing patterns” are observable across a range of natural phenomena (e.g., reptile scales [12], sand dunes [13], and zebrafish scale patterns [14]). Not only are these Turing patterns present in real-life natural phenomena, but they are also notable in that they are generally parameter-driven, uniform, and isotropic. In tactile texture generation, they would feel the same regardless of swipe direction, which implies that

they are readily distinguishable and identifiable, meaning that they can be used as discrete markers in virtual graphics. In a design context, Turing patterns have been used to enhance the aesthetics of 3-D models [15] and have demonstrated promise for use as a template for engineering materials and composites [16]. Reaction-diffusion textures have previously been used to enhance graphics on visual [17, 18] and haptic displays [19]. However, they have not been independently evaluated by the breadth of distinguishable textures they can support on these displays. We want to take advantage of the role of reaction-diffusion as a biological process by which natural textures are formed to generate recognizable, dynamic, and interesting textures on a haptic display.

### 2.3. Perceptual Space

Defining the perceptual space in which a set of textures exists allows us to visualize how distinguishable textures are within a space. A perceptual space is the n-dimensional space that defines the variability between stimuli delivered through some mode of sensory feedback. For haptic feedback, several perceptual dimensions define how individuals interpret and assess texture, around 4-5 [20]. Roughness-smoothness and hardness-softness are the most critical of these dimensions and were first identified using multi-dimensional scaling (MDS) analysis [21]. MDS analysis is a well-established method for deriving a perceptual space using either clustering methods [22, 23] or pairwise comparisons [24, 25] of texture stimuli. In this study, we want to understand the perceptual space in which reaction-diffusion textures span and to what extent. Additionally, we want to see if there is any clear relationship between the textures’ perceptual dimensions and the parameters used to generate those textures.

## 3. METHODS AND MATERIALS

### 3.1. Experimental Configuration

The experimental platform consists of a friction-modulated screen (Tanvas) that acts as a tactile platform, stage, and external monitor for the three rendering methods evaluated in this study. These methods are described in the following list:

- **Virtual Textures**, where the eight textures were rendered on a commercial friction-modulating screen and scanned using the dominant hand’s index finger.
- **Physical textures**, where the eight textures were presented as 3-D printed textures mounted on the surface and scanned using the dominant hand’s index finger.
- **Visual textures**, where the eight textures were presented using a slide show on the screen and visually inspected by the participant.

An acrylic stencil was laser-cut and adhered to the surface of the friction-modulating screen to help the user locate the virtual textures and act as a reservoir to nest the physical textures within. A visualization of the experimental setup is presented in Figure 4.

### 3.2. Texture Generation and Sample Manufacturing

The texture generation algorithm used in this study was based on the Gray-Scott model for understanding autocatalytic feedback in chemical reactors [27]. In 1993, Pearson [28] expanded

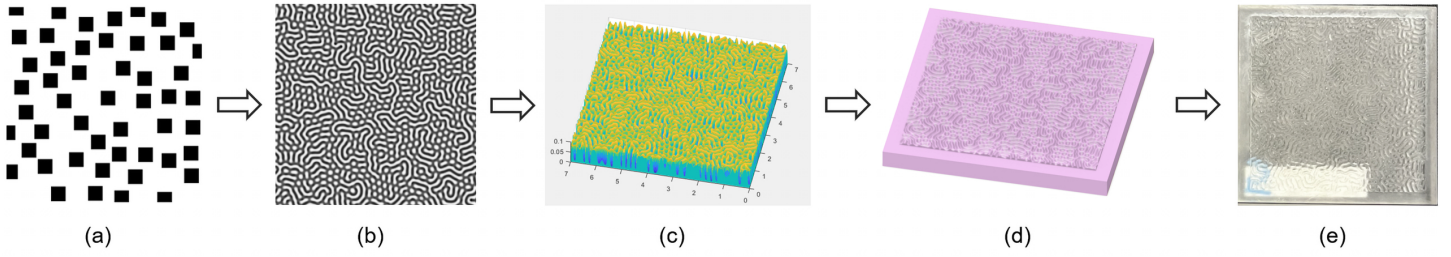


**FIGURE 1: TEXTURE GENERATION PROCESS. (A) AN INITIAL SET OF 50 STARTING POINTS WAS USED TO GENERATE A SEED IMAGE, WHICH WAS THEN EMPLOYED IN THE GRAY-SCOTT MODEL TO PRODUCE EIGHT DISTINCT TEXTURES. (B) EXAMPLE OF A 2D TEXTURE IMAGE GENERATED USING THE GRAY-SCOTT REACTION-DIFFUSION MODEL. (C) 3D MODEL CREATED IN MATLAB. (D) 3D MODEL WITH A BASEBOARD DESIGNED IN FUSION 360. (E) PHYSICAL TEXTURE FABRICATED VIA A RESIN 3D PRINTER.**

the model’s relevance to spatial self-organization, demonstrating how nonlinear interactions and finite perturbations generate complex, self-sustaining patterns. In this work, we constrained our stimulus set to 8 textures, generated from only 2 adjustable parameters (feed and kill rate). These limits ensured a small enough set of stimuli to ensure quality comparisons without fatiguing participants, while covering a wide range of parameter values to determine relationships between a given parameter and perceptual change.

The process of generating Gray-Scott reaction-diffusion textures involves three steps (see Figure 1): (i) initializing chemical concentrations, (ii) applying the Gray-Scott update formula, and (iii) converting the 2D texture image into a 3D model. For the first step, we implemented the Poisson disc sampling algorithm to generate random points in a space such that no two points are closer than a specified minimum distance. The minimum distance constraint is enforced using the Euclidean metric:

$$d(\mathbf{p}_i, \mathbf{p}_j) = \sqrt{(x_i - x_j)^2 + (y_i - y_j)^2} \geq r, \quad (1)$$

where  $\mathbf{p}_i = (x_i, y_i)$  and  $\mathbf{p}_j = (x_j, y_j)$  are distinct points in the sampling domain, and  $r$  is the minimum separation radius. We initialized 50 starting points and mapped them to a  $400 \times 400$  grid with a radius of 64 grid units to generate a default seed image, which was then employed in the Gray-Scott model to produce eight distinct isotropic textures. For each starting point, a square region of radius  $r$ , defaulting to 15 grid units, was defined to create localized disturbances (see Figure 1a).

Next, we integrated these initial conditions into the Gray-Scott reaction-diffusion model. This system describes the interaction between two chemicals,  $A$  and  $B$ , which diffuse and react according to:

$$\begin{aligned} \frac{\partial A}{\partial t} &= D_A \nabla^2 A - AB^2 + f(1 - A), \\ \frac{\partial B}{\partial t} &= D_B \nabla^2 B + AB^2 - (f + k)B, \end{aligned} \quad (2)$$

where  $A(x, y, t)$  and  $B(x, y, t)$  represent chemical concentrations,  $D_A$  and  $D_B$  are diffusion coefficients,  $f$  is the feed rate,  $k$  is the kill rate, and  $\nabla^2$  is the Laplacian operator. The discrete Laplace operator was approximated using a five-point stencil:

$$\nabla^2 M_{ij} \approx \frac{1}{h^2} [M_{i+1,j} + M_{i-1,j} + M_{i,j+1} + M_{i,j-1} - 4M_{ij}], \quad (3)$$

where  $h$  is the grid spacing (set to 1 in pixel-based simulations).

The generated textures depend primarily on the feed ( $f$ ) and kill rate ( $k$ ) parameters. All other parameters were kept constant:  $D_A = 0.14$  and  $D_B = 0.07$  based on the suggestion from [26]. The simulation ran for 40,000 iterations to ensure that all texture images were stable, using the same seed image with 50 starting points to guarantee isotropic textures. The adjusted feed ( $f$ ) and kill rate ( $k$ ) parameters were carefully distributed throughout the K-F log curve in the phase diagram of the isotropic Gray-Scott model to generate a set of 8 distinct texture images (see Figure 2). The resultant textures were uniform, periodic, and isotropic grayscale patterns.

The final step involved converting 2D texture images into 3D printable models to enable tactile evaluation by participants. The workflow (Figure 1c) began by storing the 2D texture heightmap as a matrix in a CSV file, which was then scaled to physical dimensions of  $70 \times 70 \times 1$  mm. A triangular surface mesh was generated via Delaunay triangulation on the gridded  $X-Y$  coordinates, with  $Z$ -values defining vertex heights. This triangulation was exported as a text-based STL file using MATLAB’s triangulation and stlwrite functions. To ensure printability, the STL file was imported into Fusion 360, where an  $80 \times 80 \times 6$  mm baseboard was added beneath the texture. The finalized model was fabricated using a clear photopolymer resin on a Formlabs Form 4 stereolithography (SLA) 3D printer (see Figure 1e and Figure 3).

### 3.3. Data Analysis

We collected pairwise dissimilarity ratings between texture stimuli to assess the breadth of distinct textures that reaction-diffusion can generate across different sensory modes. Dissimilarity ratings within each experimental set were normalized to a 0-1 scale across all subjects to account for each participant’s subjective rating scale.

The ratings were then arranged into the dissimilarity matrices, which were used as inputs for our NMDS analysis. We used NMDS because we were interested in the relative distance and relationships between the eight textures. We confirmed goodness-of-fit using a Kruskal stress curve, identified distinct clusters using a combination of the NMDS plots and a dendrogram to clarify them, and then plotted the dissimilarity measures against the control parameters (i.e., Feed rate, Kill rate).

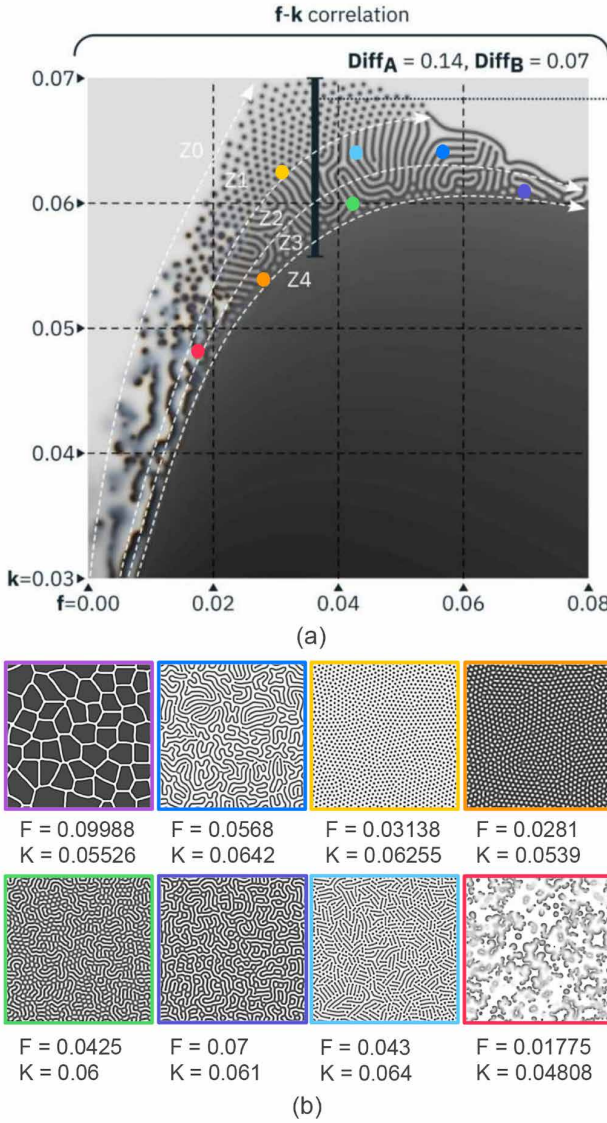


**FIGURE 2: EIGHT REACTION-DIFFUSION TEXTURES.** (A) PHASE DIAGRAM FOR THE ISOTROPIC GRAY-SCOTT MODEL, WHERE EIGHT DIFFERENTLY COLORED DOTS CORRESPOND TO EIGHT UNIQUE REACTION-DIFFUSION TEXTURES. THE ORIGINAL PLOT IS ADAPTED FROM [26]. (B) PANEL SHOWING THE EIGHT REACTION-DIFFUSION TEXTURES EVALUATED IN THIS STUDY, INCLUDING THEIR ASSOCIATED FEED ( $f$ ) AND KILL RATE ( $k$ ) PARAMETERS.

#### 4. PARTICIPANT STUDY

In this study, a total of 7 participants (4 women, ages 22–34) were evaluated. This study was approved by the Institutional Review Board of Texas A&M University (IRB2024-0539), and participants were compensated for their participation.

##### 4.1. Tactile Acuity Assessment and Training Session

Before the main study, participants were tested on their ability to discriminate between textures of variable spatial frequency on a friction-modulating screen and to become familiar with the virtual texture platform, as most had never interacted with one. This ensured that they could effectively interpret the surface's mode of

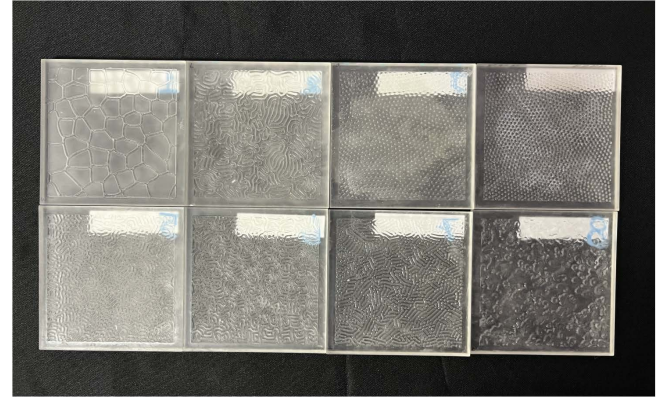


**FIGURE 3: 3D-PRINTED PHYSICAL TEXTURE SAMPLES.** RESIN 3D-PRINTED TEXTURE SAMPLES USED FOR THE PHYSICAL PERCEPTION MODALITY.

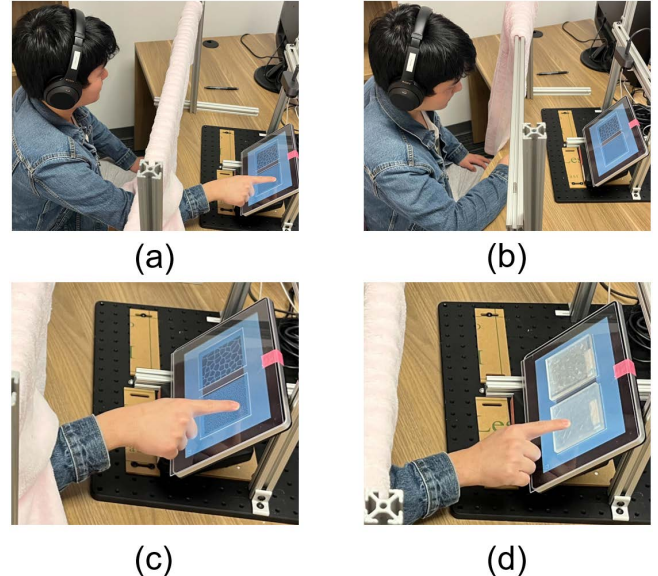


**FIGURE 4: EXPERIMENTAL SETUP.** (A) TACTILE INTERACTION MODE WITH CURTAIN OBSCURING VIEW OF EXPERIMENTAL SETUP. (B) VISUAL INTERACTION MODE WITH CURTAIN DRAWN TO PROVIDE FULL VIEW OF EXPERIMENTAL SETUP. (C) EXPLORATION OF VIRTUAL TEXTURES USING THE DOMINANT HAND'S INDEX FINGER. (D) EXPLORATION OF PHYSICAL TEXTURES USING THE DOMINANT HAND'S INDEX FINGER.

tactile feedback. To assess each participant, we generated three textures with variable spatial frequency (.05, .5, one cycle/pixel) that were then presented as a series of pairs that participants were asked to rate in terms of dissimilarity.

In addition to testing tactile acuity for virtual textures, participants were briefed on using a free magnitude rating scale, a well-established method for pairwise comparisons of stimuli [29, 30]. When evaluating each texture pair, participants were instructed to arbitrarily choose their initial rating and rate all subsequent pairs relative to this baseline value. Participants were instructed on how to interact with each texture—that is, they were told to scan the surface of the tactile texture samples using their dominant

hand's index finger. If they tapped on the surface or used more than one finger, they were corrected by the supervising researcher. These training textures were not reused at any other point in the study.

#### 4.2. Dissimilarity Ratings

Participants were randomly assigned one of the three rendering methods (visual, virtual, and physical textures). Additionally, the 28 texture pairs were the same but randomly sorted. When participants used tactile feedback, an opaque curtain obscured the experimental platform. For the virtual texture experiment, participants were asked to wear noise-canceling headphones playing pink noise to isolate touch as the primary mode of sensory feedback.

Participants were asked to scan two adjacent textures and rate the dissimilarity of these textures across a series of 28 pairs of textures for each rendering method. They were asked to ensure that this rating was greater than zero, but that these ratings could be as large or small as they wanted. Participants were told that each initial rating for an experimental set was arbitrary and that all subsequent ratings would be made as a ratio pair (e.g., if a subsequent pair is twice as dissimilar, the resultant rating would be twice as large). For every 10 ratings, they were asked to take a 1-minute break before progressing to the next pair. Between experimental sets, they were asked to take a 3-minute break. When each participant completed each set of 28 ratings and progressed to another rendering method, they were asked to ignore all prior ratings.

Immediately adjacent to the experimental setup was a laptop with a GUI for participants to record their dissimilarity ratings for each texture pair. Once they had successfully evaluated and rated a texture pair, the supervising researcher exchanged it for another texture pair and moved on to the next trial. At the end of the study, each participant evaluated 84 texture pairs across all three rendering methods.

### 5. RESULTS

We rendered and manufactured a set of eight distinct textures using a reaction-diffusion algorithm. We varied two controllable parameters (the Kill and Feed rates) and held all other variables constant. The Feed rate ( $F$ ) refers to the consumption of material added to the reaction, while the Kill rate ( $K$ ) refers to the removal of material generated by the reaction. We wanted to determine how distinctive each texture was and the relationship between perceived dissimilarity and the two control parameters. Our group performed three experiments in a psychophysical study to evaluate the breadth of perceptual space these textures occupied across different modes of interaction.

Participants evaluated the dissimilarity of a set of eight reaction-diffusion textures using (1) visual evaluation, (2) sliding touch along a physical texture, and (3) sliding touch on a virtual texture rendered using a friction-modulating screen. Participants rated the dissimilarity of each texture pair, and their final ratings were analyzed using non-metric MDS (NMDS) analysis. The 3-D NMDS plots are visualized in Figure 5. We used these plots to identify a possible relationship between the control parameters and perception.

#### 5.1. Perception of Reaction-Diffusion Textures using Visual Feedback

Inspection of the NMDS data for the experiment using visual feedback indicates:

- Textures 1-8 appear to form distinct corners of a prism-like distribution in the 3D NMDS output.
- Textures 8, 6, 4, and 1 form a 'face'. Textures 3, 7, 5, and 2 follow a similar configuration.
- Textures 6 and 4 appear to form a cluster.
- Textures 1 and 8 appear to be outliers.

The textures do not appear to be arranged according to their reaction-diffusion control parameters, but there seems to be some relationship between feature size and how dark the image is. This data is visualized in Figures 5 and 6. The arrangement of the textures in dimensions 1 and 2 seems to correspond to both average shade and the presence of distinct shape geometries, with dimension 1 corresponding to the former and dimension 2 to the latter. The effects of dimension 3 are less clear but seem related to the geometries of the embedded features and the space they occupy.

A dendrogram was used to visualize the groupings and support these texture grouping assessments; however, it also implies that there may be a cluster between textures 5 and 7 and a gradient consisting of textures 4-7. Additionally, it identifies a possible cluster between 2 and 3. Overall, there is a balanced relationship between the eight textures, with some weak similarities between select pairs of textures.

We evaluated the relationship between four different metrics and the participant dissimilarity ratings. We calculated the  $R^2$  value to determine the strength of the relationship between the predictors and their response variables. We then calculated the p-value to determine if the assigned relationship was statistically significant. For each metric, there is no relationship with the Kill rate ( $R^2 = 0.0523$ ) and no relationship with the Feed rate ( $R^2 = 0.0180$ ). A visualization of the relationship between these different metrics and dissimilarity is shown in Figure 7.

#### 5.2. Perception of Physical Reaction Diffusion Textures using Tactile Feedback

Inspection of the NMDS data for the experiment using tactile feedback on a physical surface indicates:

- Textures 1, 2, 3, and 5 seem to form a cluster gradient.
- Textures 3, 5, 6, and 7 seem to form a gradient.
- Textures 6 and 7 seem to form a possible cluster.
- Textures 4 and 8 appear to be outliers.

This data is visualized in Figures 5 and 8. From the 2-D projections of the 3-D NMDS, Dimension 1 seems to correspond to the Kill rate. A dendrogram was used to visualize the groupings and support these texture grouping assessments.

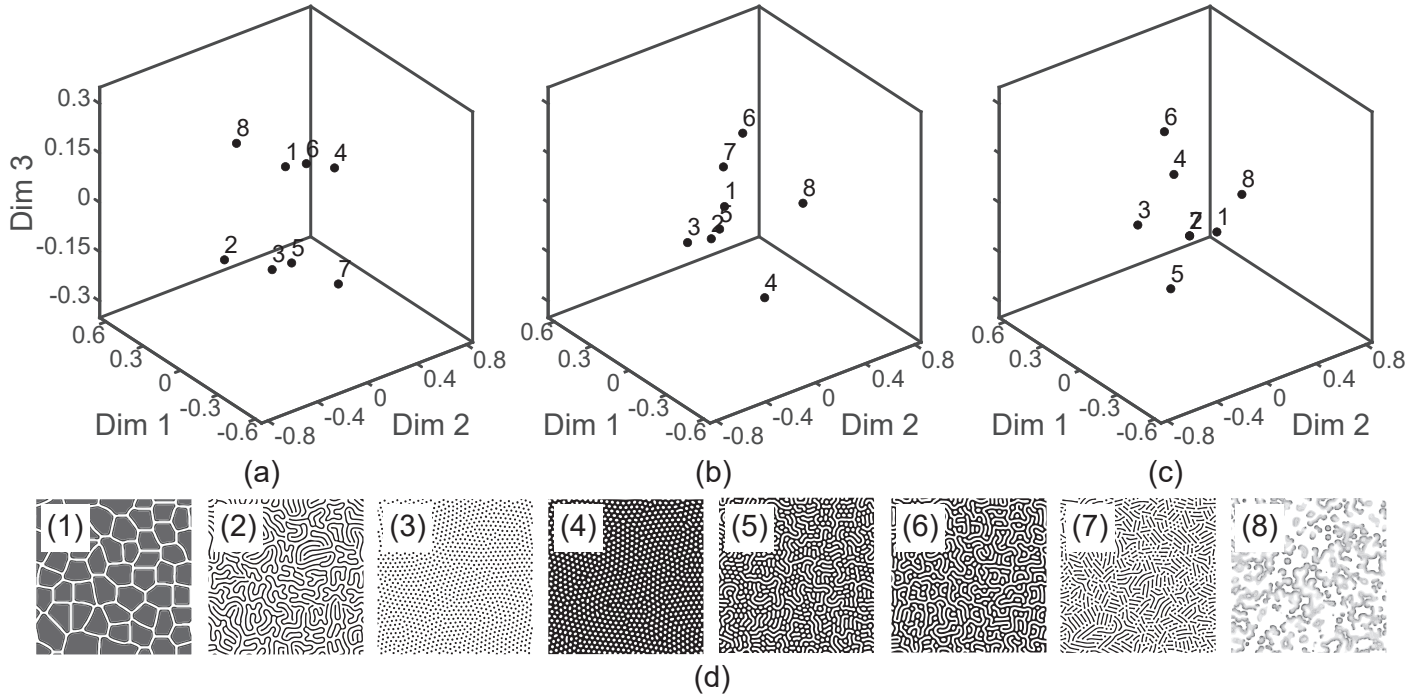


**FIGURE 5: 3-D NMDS RESULTS. ILLUSTRATION OF THE (A) VISUAL, (B) PHYSICAL, (C) AND VIRTUAL NMDS 3-D PLOTS OF PARTICIPANT DISSIMILARITY RATINGS, AS WELL AS (D) A KEY MAPPING EACH OF THE TESTED TEXTURES TO A VALUE IN EACH PLOT.**

We evaluated the relationship between two different metrics and the participant dissimilarity ratings. We calculated the  $R^2$  statistic to measure the relationship between a predictor and response variables. We then calculated the p-value to determine whether the assigned relationship was statistically significant. For each metric, there is a strong relationship with the Kill rate ( $R^2 = 0.2536$ ) and a weak relationship with the Feed rate ( $R^2 = 0.1011$ ).

A visualization of the relationship between these different metrics and dissimilarity is shown in Figure 9. The results here imply that the Kill rate significantly affects the tactile perception of dissimilarity. This is consistent with how the textures were clustered in the NMDS data.

### 5.3. Perception of Virtual Reaction Diffusion Textures using Tactile Feedback

Inspection of the nonmetric NMDS data for the experiment using tactile feedback on a virtual surface indicates:

- Textures 1, 2, and 7 seem to form a weak cluster.
- Textures 2 and 7 overlap.
- Textures 6, 4, 3, and 5 follow a dissimilarity gradient.
- Texture 8 is an outlier.

Otherwise, there does not appear to be a clear clustering of textures, and they seem to be perceived as equally similar or dissimilar. This data is visualized in Figures 5 and 10. A dendrogram was used to visualize the groupings and support these initial texture grouping assessments, but it seems to indicate that both 1 and 8 are outliers.

We evaluated the relationship between two different metrics and the participant dissimilarity ratings. We calculated (1) the  $R^2$  statistic to determine the strength of the relationship between a predictor and the response variables and (2) the p-value to determine whether the assigned relationship was statistically significant. For each metric, there is a weak relationship with the Kill rate ( $R^2 = 0.1448$ ) and no relationship with the Feed rate ( $R^2 = 0.0551$ ). A visualization of the relationship between these different metrics and dissimilarity is shown in Figure 11.

The overlap of textures 2 and 7; a very weak—but more precisely organized when compared to the physical textures—gradient of textures 6, 4, 3, and 5; and the outliers of 1 and 8 indicate that the feature geometry might also be a factor in similarity judgments. That is, the textures also seem to be organized based on whether there are distinct geometries (like the curves in textures 2 or 7) or if there are clusters of dots (like the cluster gradient with textures 3–6). As for how the outliers could be differentiated, texture 1 has large and distinct shape objects, and 8 is a non-binary texture—that is, it has a gradient of friction values that can readily distinguish it from the other textures.

## 6. DISCUSSION

We studied the visual and tactile perception of dissimilarity between textures generated using a reaction-diffusion algorithm. Our goal was to determine whether there is a direct link between the parameters that control the makeup of a reaction-diffusion texture and some perceptual dimension. We also wanted to determine whether the resultant textures were dissimilar enough to be individually identified (i.e., if they covered a significant breadth of the sensory modes' perceptual space).

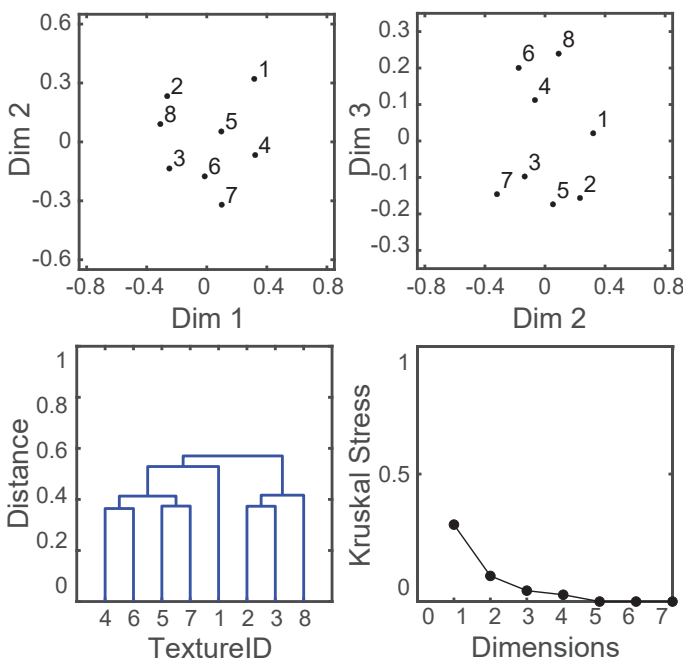


**FIGURE 6: VISUAL NMDS RESULTS.** A 2-D PROJECTION OF THE 3-D NMDS RESULTS WAS USED TO VERIFY THE PRESENCE OF CLUSTERS AND GRADIENTS ALONG THE DIFFERENT DIMENSIONS. A DENDROGRAM WAS USED TO VERIFY IDENTIFIED CLUSTERS AND THE PRESENCE OF OUTLIERS, AND A SCREE PLOT WAS USED TO IDENTIFY THE APPROPRIATE NUMBER OF DIMENSIONS FOR THE NMDS ANALYSIS.

### 6.1. Perception of Reaction-Diffusion Textures using Visual Feedback

When participants evaluated the texture patterns using vision, there was no relationship between the controllable parameters and their dissimilarity assessments. This indicates that the controllable parameters, in this case, are not well suited for adjusting texture properties along some perceptual dimension due to the absence of a clear relationship between the main assessors of dissimilarity and those parameters. Several participants commented on the overall shade of the textures and feature sizes, suggesting relevant parameters for future analysis.

### 6.2. Perception of Reaction-Diffusion Textures using Tactile Feedback

When participants used tactile feedback during sliding touch on *physical smaples*, we found a strong relationship between tactile perception of dissimilarity and the Kill rate and a weak relationship between tactile perception of dissimilarity and the Feed rate. A weaker, but still present, relationship between the Kill rate and dissimilarity was observed with the virtual friction-modulated textures. These results indicate that the control parameters effectively and predictably affect user perception of dissimilarity during sliding touch, but that this relationship is more subtle on virtual surfaces. Larger changes in both parameters may be necessary to create tactiley distinct textures when using friction modulation as a feedback mode.

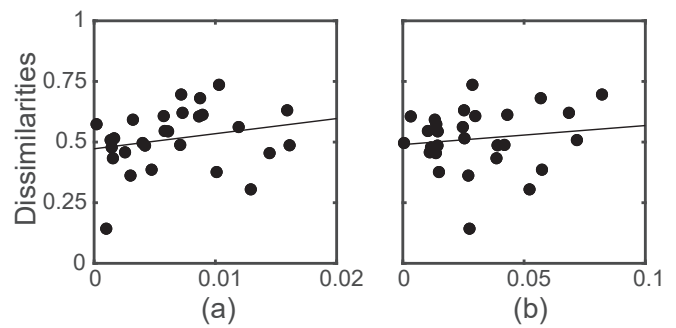


**FIGURE 7: VISUAL SAMPLE METRICS. (A) KILL RATE, (B) FEED RATE.**

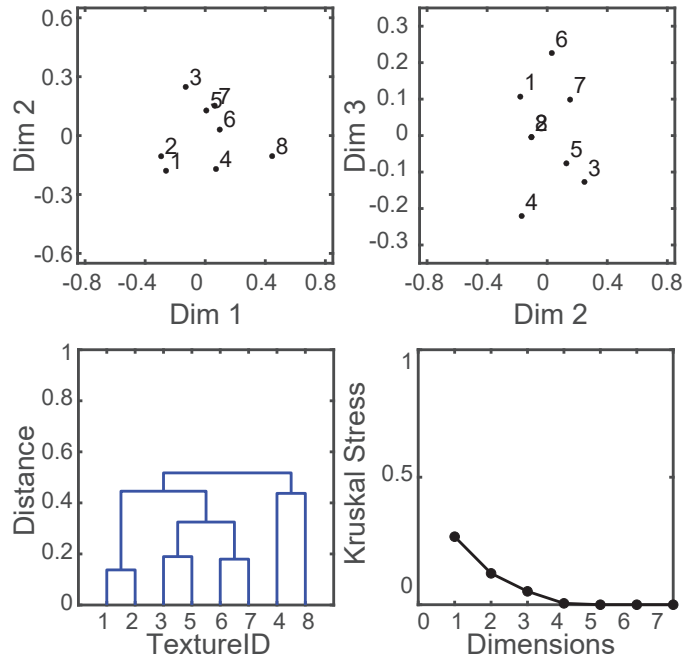


**FIGURE 8: PHYSICAL NMDS RESULTS.** A 2-D PROJECTION OF THE 3-D NMDS RESULTS WAS USED TO VERIFY THE PRESENCE OF CLUSTERS AND GRADIENTS ALONG THE DIFFERENT DIMENSIONS. A DENDROGRAM WAS USED TO VERIFY IDENTIFIED CLUSTERS AND THE PRESENCE OF OUTLIERS, AND A SCREE PLOT WAS USED TO IDENTIFY THE APPROPRIATE NUMBER OF DIMENSIONS FOR THE NMDS ANALYSIS.

### 6.3. Study Limitations and Future Work

Our goal was to determine whether reaction-diffusion algorithms could present a method through which touchscreen users could control the impression of a texture by adjusting parameters that intuitively correspond to some perceptual dimension. Our results show that this is true for both the physical and virtual methods of communicating texture information. The relationship between the reaction-diffusion control parameters and tactile perception of dissimilarity must be more closely examined within a broader texture library to understand these textures' perceptual dimensions.

Another limitation of this study is that we only investigated

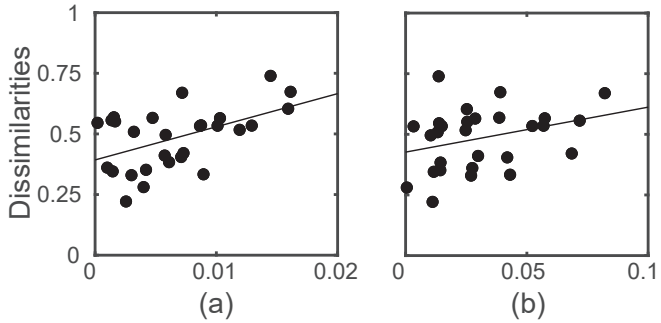


**FIGURE 9: PHYSICAL SAMPLE METRICS. (A) KILL RATE, (B) FEED RATE.**

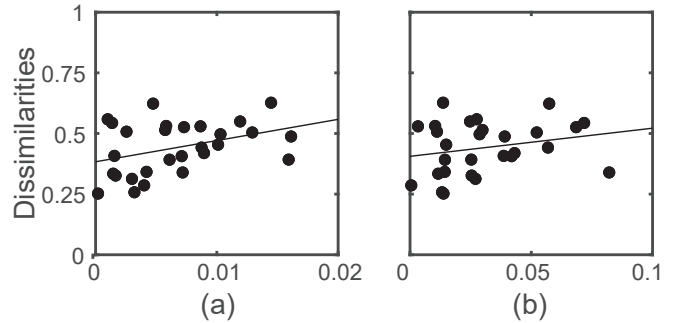


**FIGURE 11: VIRTUAL SAMPLE METRICS.(A) KILL RATE, (B) FEED RATE.**

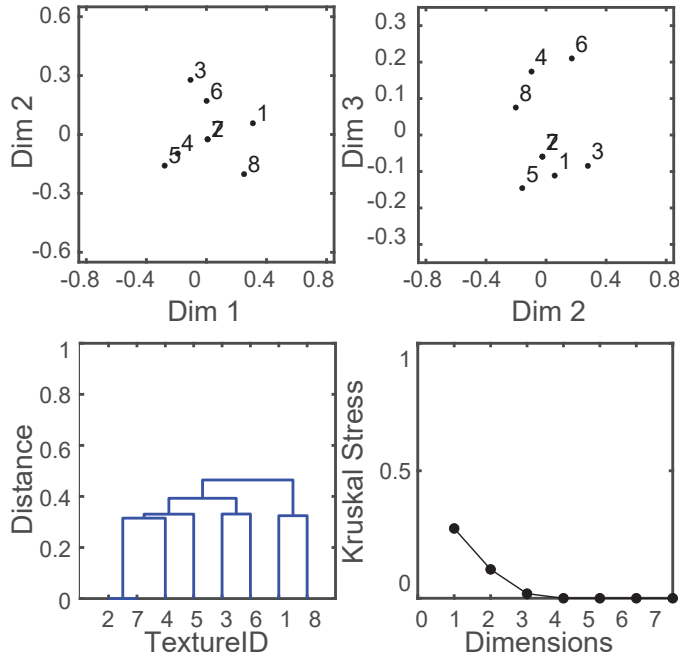


**FIGURE 10: VIRTUAL NMDS RESULTS. A 2-D PROJECTION OF THE 3-D NMDS RESULTS WAS USED TO VERIFY THE PRESENCE OF CLUSTERS AND GRADIENTS ALONG THE DIFFERENT DIMENSIONS. A DENDROGRAM WAS USED TO VERIFY IDENTIFIED CLUSTERS AND THE PRESENCE OF OUTLIERS, AND A SCREE PLOT WAS USED TO IDENTIFY THE APPROPRIATE NUMBER OF DIMENSIONS FOR THE NMDS ANALYSIS.**

the feed ( $f$ ) and kill rates ( $k$ ) of our reaction-diffusion model. Several other parameters remain underexplored. For instance, varying the number of starting points alters the minimum distance constraints, potentially resulting in anisotropic textures. Similarly, adjusting the radius of the square region around each starting point can introduce more or less localized disturbances in the seed image, thereby influencing the spatial frequency of the resulting patterns. Additionally, modifying the diffusion coefficients ( $D_A$  and  $(D_B)$ ) affects the scale of the patterns while preserving their overall characteristics.

Psychophysical experiments collected coarse information on whether the textures spanned some perceptual space using NMDS

and whether there were relationships between the control parameters and user perception of dissimilarity. To better understand the most salient properties of these textures and their relationship with perception, our future analysis will look for the strength of different texture features, such as average feature height or spatial frequency, in predicting texture similarity ratings. These parameters for visual textures link directly to features in haptic textures, such as average height or pattern density. By calculating these values, we will better understand how our control parameters influence tactile perception.

Furthermore, we acknowledge that our participant count ( $N=7$ ) may limit the statistical significance of our results. Future work will expand recruitment to strengthen the results reported in this work.

## 7. CONCLUSION

This study evaluated the perceptual dimensions in which parameter-controlled reaction-diffusion textures span three sensory feedback modes. The visual perceptual experiment showed no dependency on the control parameters when assessing dissimilarity between textures. In contrast, tactile perception of dissimilarity for both physical and virtual textures depended on the control parameters, with the latter being affected more subtly by differences in the Kill rate parameter.

These results indicate that reaction-diffusion parameters are well suited for applications on haptic surface displays and that the different control parameters moderately predict texture perception of dissimilarity for physical and virtual textures. This makes texture generation more accessible to a wider audience of designers, as non-expert users can intuitively generate a range of unique, customizable textures using these parameters. Future work will look for the most salient perceived features underlying these design parameters and the relative advantage of reaction-diffusion for texture generation.

## REFERENCES

- [1] Osgouei, Reza Haghghi, Kim, Jin Ryong and Choi, Seungmoon. "Data-Driven Texture Modeling and Rendering on Electrovibration Display." *IEEE Transactions on Haptics* Vol. 13 No. 2 (2020): pp. 298–311. DOI [10.1109/TOH.2019.2932990](https://doi.org/10.1109/TOH.2019.2932990).
- [2] Culbertson, Heather, Unwin, Juliette and Kuchenbecker, Katherine J. "Modeling and Rendering Realistic Tex-

- tures from Unconstrained Tool-Surface Interactions.” *IEEE Transactions on Haptics* Vol. 7 No. 3 (2014): pp. 381–393. DOI [10.1109/TOH.2014.2316797](https://doi.org/10.1109/TOH.2014.2316797).
- [3] Hassan, Waseem, Abdulali, Arsen and Jeon, Seokhee. “Authoring New Haptic Textures Based on Interpolation of Real Textures in Affective Space.” *IEEE Transactions on Industrial Electronics* Vol. 67 No. 1 (2020): pp. 667–676. DOI [10.1109/TIE.2019.2914572](https://doi.org/10.1109/TIE.2019.2914572).
- [4] Vasudevan, Hari and Manivannan, M. “Recordable Haptic textures.” *2006 IEEE International Workshop on Haptic Audio Visual Environments and their Applications (HAVE 2006)*: pp. 130–133. 2006. DOI [10.1109/HAVE.2006.283779](https://doi.org/10.1109/HAVE.2006.283779).
- [5] Meyer, David J., Peshkin, Michael A. and Colgate, J. Edward. “Tactile Paintbrush: A procedural method for generating spatial haptic texture.” *2016 IEEE Haptics Symposium (HAPTICS)*: pp. 259–264. 2016. DOI [10.1109/HAPTICS.2016.7463187](https://doi.org/10.1109/HAPTICS.2016.7463187).
- [6] Manfredi, Louise R., Saal, Hannes P., Brown, Kyler J., Zielinski, Mark C., Dammann, John F., Polashock, Vicky S. and Bensmaia, Sliman J. “Natural scenes in tactile texture.” *Journal of Neurophysiology* Vol. 111 No. 9 (2014): pp. 1792–1802. DOI [10.1152/jn.00680.2013](https://doi.org/10.1152/jn.00680.2013). URL <https://doi.org/10.1152/jn.00680.2013>, URL <https://doi.org/10.1152/jn.00680.2013>. PMID: 24523522.
- [7] Janko, Marco, Primerano, Richard and Visell, Yon. “On Frictional Forces between the Finger and a Textured Surface during Active Touch.” *IEEE Transactions on Haptics* Vol. 9 No. 2 (2016): pp. 221–232. DOI [10.1109/TOH.2015.2507583](https://doi.org/10.1109/TOH.2015.2507583).
- [8] Halabi, Osama and Khattak, Gulruk. “Generating haptic texture using solid noise.” *Displays* Vol. 69 (2021): p. 102048. DOI <https://doi.org/10.1016/j.displa.2021.102048>. URL <https://www.sciencedirect.com/science/article/pii/S0141938221000597>.
- [9] Shopf, Jeremy and Olano, Marc. “Procedural haptic texture.” *Proceedings of the 19th Annual ACM Symposium on User Interface Software and Technology*: p. 179–186. 2006. Association for Computing Machinery, New York, NY, USA. DOI [10.1145/1166253.1166281](https://doi.org/10.1145/1166253.1166281). URL <https://doi.org/10.1145/1166253.1166281>.
- [10] Fritz, Jason P. and Barner, Kenneth E. “Stochastic models for haptic texture.” Stein, Matthew R. (ed.). *Telemanipulator and Telepresence Technologies III*, Vol. 2901: pp. 34 – 44. 1996. International Society for Optics and Photonics, SPIE. DOI [10.1117/12.263011](https://doi.org/10.1117/12.263011). URL <https://doi.org/10.1117/12.263011>.
- [11] Turing, Alan Mathison. “The chemical basis of morphogenesis.” *Philosophical Transactions of the Royal Society of London. Series B, Biological Sciences* Vol. 237 No. 641 (1952): pp. 37–72. DOI [10.1098/rstb.1952.0012](https://doi.org/10.1098/rstb.1952.0012). URL <https://royalsocietypublishing.org/doi/pdf/10.1098/rstb.1952.0012>, URL <https://royalsocietypublishing.org/doi/abs/10.1098/rstb.1952.0012>.
- [12] Fofonjka, Anamarija and Milinkovitch, Michel C. “Reaction-diffusion in a growing 3D domain of skin scales generates a discrete cellular automaton.” *Nature Communications* Vol. 12 No. 1 (2021): p. 2433.
- [13] Ball, Philip. “In retrospect: the physics of sand dunes.” (2009).
- [14] Nakamasu, Akiko, Takahashi, Go, Kanbe, Akio and Kondo, Shigeru. “Interactions between zebrafish pigment cells responsible for the generation of Turing patterns.” *Proceedings of the National Academy of Sciences* Vol. 106 No. 21 (2009): pp. 8429–8434. DOI [10.1073/pnas.0808622106](https://doi.org/10.1073/pnas.0808622106). URL <https://www.pnas.org/doi/pdf/10.1073/pnas.0808622106>, URL <https://www.pnas.org/doi/abs/10.1073/pnas.0808622106>.
- [15] Francesca, Bertacchini, Roberto, Beneduci, Eleonora, Bilotta, Francesco, Demarco, Pietro, Pantano and Carmelo, Scuro. “Mathematical pattern for parametric design: the case study of Grey-Scott cross diffusion model.” *Procedia Computer Science* Vol. 217 (2023): pp. 756–764. DOI <https://doi.org/10.1016/j.procs.2022.12.272>. URL <https://www.sciencedirect.com/science/article/pii/S187705092202350X>. 4th International Conference on Industry 4.0 and Smart Manufacturing.
- [16] Tanaka, Masato, Montgomery, S. Macrae, Yue, Liang, Wei, Yaochi, Song, Yuyang, Nomura, Tsuyoshi and Qi, H. Jerry. “Turing pattern-based design and fabrication of inflatable shape-morphing structures.” *Science Advances* Vol. 9 No. 6 (2023): p. eade4381. DOI [10.1126/sciadv.ade4381](https://doi.org/10.1126/sciadv.ade4381). URL <https://www.science.org/doi/pdf/10.1126/sciadv.ade4381>, URL <https://www.science.org/doi/abs/10.1126/sciadv.ade4381>.
- [17] Turk, Greg. “Generating textures on arbitrary surfaces using reaction-diffusion.” *AcM Siggraph Computer Graphics* Vol. 25 No. 4 (1991): pp. 289–298.
- [18] Witkin, Andrew and Kass, Michael. “Reaction-diffusion textures.” *Proceedings of the 18th annual conference on Computer graphics and interactive techniques*: pp. 299–308. 1991.
- [19] Ho, Chih-Hao, Basdogan, Cagatay and Srinivasan, Mandayam A. “Efficient Point-Based Rendering Techniques for Haptic Display of Virtual Objects.” *Presence: Teleoperators and Virtual Environments* Vol. 8 No. 5 (1999): pp. 477–491. DOI [10.1162/105474699566413](https://direct.mit.edu/pvar/article-pdf/8/5/477/1623291/105474699566413.pdf). URL <https://direct.mit.edu/pvar/article-pdf/8/5/477/1623291/105474699566413.pdf>, URL <https://doi.org/10.1162/105474699566413>.
- [20] Okamoto, Shogo, Nagano, Hikaru and Yamada, Yoji. “Psychophysical Dimensions of Tactile Perception of Textures.” *IEEE Transactions on Haptics* Vol. 6 No. 1 (2013): pp. 81–93. DOI [10.1109/TOH.2012.32](https://doi.org/10.1109/TOH.2012.32).
- [21] Hollins, Mark, Faldowski, Richard, Rao, Suman and Young, Forrest. “Perceptual dimensions of tactile surface texture: A multidimensional scaling analysis.” *Perception & psychophysics* Vol. 54 (1993): pp. 697–705.
- [22] Friesen, Rebecca Fenton, Klatzky, Roberta L., Peshkin, Michael A. and Colgate, J. Edward. “Building a navigable fine texture design space.” *IEEE Transactions on Haptics* Vol. 14 No. 4 (2021): pp. 897–906.

- [23] Hwang, Inwook, Yun, Sungryul and Park, Jaeyoung. "Perceptual space and adjective rating of 2.5 D tactile patterns." *Scientific Reports* Vol. 15 No. 1 (2025): p. 4244.
- [24] Sahli, Riad, Prot, Aubin, Wang, Anle, Müser, Martin H, Piovarči, Michal, Didyk, Piotr and Bennewitz, Roland. "Tactile perception of randomly rough surfaces." *Scientific reports* Vol. 10 No. 1 (2020): p. 15800.
- [25] Yoshioka, Takashi, Bensmaia, Sliman J, Craig, Jim C and Hsiao, Steven S. "Texture perception through direct and indirect touch: An analysis of perceptual space for tactile textures in two modes of exploration." *Somatosensory & motor research* Vol. 24 No. 1-2 (2007): pp. 53–70.
- [26] Zomparelli, Alessandro and Naboni, Roberto. "Generative design of isostatic ribbed slabs using anisotropic Reaction-Diffusion." *Proceedings of IASS Annual Symposia*, Vol. 2023. 18: pp. 1–12. 2023. International Association for Shell and Spatial Structures (IASS).
- [27] Gray, Peter and Scott, Stephen K. "Autocatalytic reactions in the isothermal, continuous stirred tank reactor: Oscillations and instabilities in the system  $A + 2B \rightarrow 3B; B \rightarrow C$ ." *Chemical Engineering Science* Vol. 39 No. 6 (1984): pp. 1087–1097.
- [28] Pearson, John E. "Complex patterns in a simple system." *Science* Vol. 261 No. 5118 (1993): pp. 189–192.
- [29] Gescheider, GA. "Psychophysics: The fundamentals." (2013).
- [30] Boundy-Singer, Zoe M, Saal, Hannes P and Bensmaia, Sliman J. "Speed invariance of tactile texture perception." *Journal of neurophysiology* Vol. 118 No. 4 (2017): pp. 2371–2377.